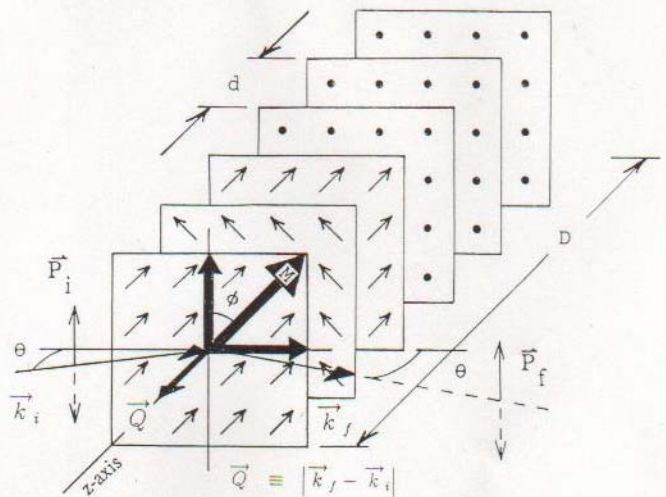
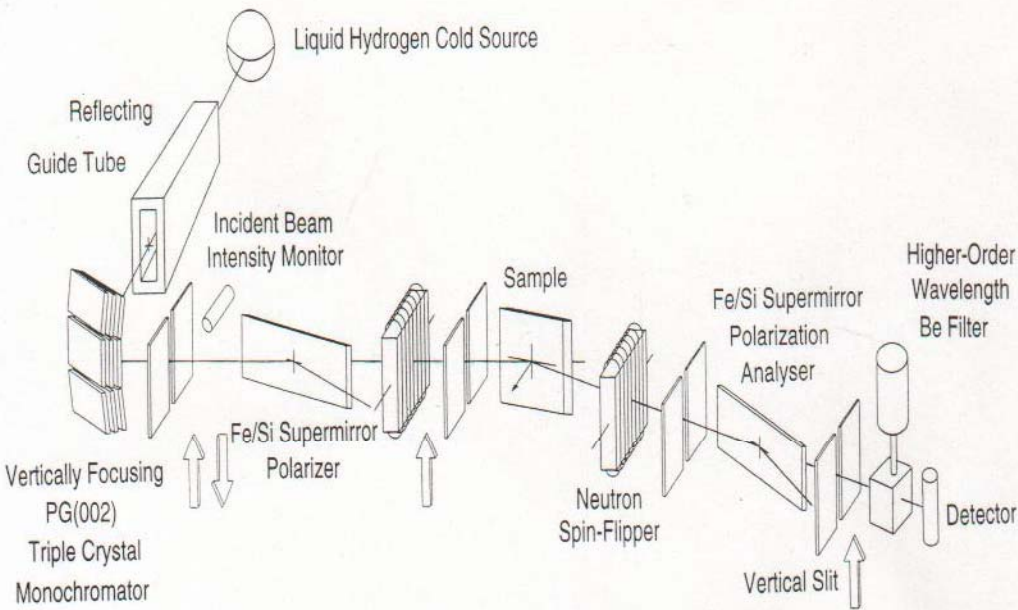


National School on Neutron and X-ray Scattering

August 15-29, 2004

Argonne National Laboratory

Magnetic Scattering I: Fundamentals



C.F.Majkrzak

National Institute of Standards and Technology

THE PRINCIPLES OF MAGNETIC SCATTERING

6.1. Introduction

At the beginning of Chapter 2 we explained that, whereas in general the scattering of neutrons by atoms was a nuclear process, nevertheless an exception occurred with magnetic atoms, in the case of which there is additional scattering on account of an interaction between the neutron magnetic moment and the magnetic moment of the atom. We return in this chapter to a discussion of the principles of magnetic scattering and will proceed in the following two chapters to a detailed account of magnetic form-factors and of the way particular types of magnetic structure are revealed.

The determination of the magnetic structures of materials is a task which can be achieved only by making measurements of the scattering of neutrons. Indeed it is true to say that our whole conception of the existence of a 'magnetic architecture' within the atomic structure of solids has arisen from observations with neutrons.

The elements of the first transition series which includes iron, cobalt, and nickel, have incomplete 3d shells, as indicated in Table 12 which lists the electronic structures of the free atoms with atomic numbers 19–30. The arrangements of the 3d and 4s shells of some free atoms and ions are shown in Table 13 which also gives the number of unpaired electrons and the spectroscopic ground terms of the ions. These unpaired electrons give rise to a resultant magnetic moment. Interaction of this with the magnetic moment of the neutron, which has a spin quantum number of $\frac{1}{2}$ and a magnetic moment of 1.9 nuclear magnetons, produces neutron scattering which is additional to that produced by the nucleus.

It is worth noting in passing that the fact the neutron, which is an uncharged particle, possesses a magnetic moment is anomalous. A likely explanation is that a neutron spends part of its time dissociated into a proton and a negative π -meson, and although the centres of their respective positive and negative charges do coincide yet the negative charge is more diffuse. This would cause the neutron

POLARIZED NEUTRON REFLECTOMETRY

C.F.Majkrzak (National Institute of Standards and Technology)

Historically, neutron elastic scattering studies have provided a wealth of important atomic scale information about the magnetic structures of condensed matter, a significant part of which could not have been obtained by any other means. In the beginning, magnetic neutron diffraction research was performed primarily on bulk crystals. In more recent years, advances in thin film deposition techniques have made it possible to synthesize a variety of new types of layered magnetic systems, with properties that can be tailored for studies of fundamental scientific interest as well as technological applications. Throughout this still ongoing development, neutron scattering techniques, especially polarized neutron reflectometry (PNR) and diffraction, have made and continue to make significant contributions to the understanding of the physical behavior of magnetic thin films and superlattices (see, for example, the references [1,2]).

Polarized neutron reflectometry can be divided into two broad categories, one of which corresponds to reflection measurements performed with the wavevector transfer Q normal to the film surface, commonly referred to as specular reflectometry, and the other to scattering done with some component of Q lying in the plane of the film. Analysis of the specular polarized neutron reflectivity, measured as a function of Q , yields the in-plane average of the vector magnetization depth profile along the surface normal, with a spatial resolution of less than a nanometer in certain cases. The nonspecular reflectivity, on the other hand, reveals in-plane magnetic structure, such as that associated with domains or artificially patterned surfaces.

In this presentation, we will first show why PNR is such an extraordinarily sensitive, and in some regards unique, probe of magnetic order in thin films and multilayers. We will also illustrate how state-of-the-art methods in experimental and theoretical PNR (see, for example, [3]) can be applied to study current problems in magnetism, including investigations of magnetic semiconductor films and superlattices [4], of particular interest in the relatively new field of "spintronics".

References

1. C.F.Majkrzak, J.Kwo, M.Hong, Y.Yafet, D.Gibbs, C.L.Chien, and J.Bohr, *Advances in Physics* **40**, 99 (1991).
2. M.R.Fitzsimmons, S.D.Bader, J.A.Borchers, G.P.Felcher, J.K.Furdyna, A.Hoffmann, J.B.Kortright, I.K.Schuller, T.C.Schulthess, S.K.Sinha, M.F.Toney, D.Weller, and S.Wolf, *Journal of Magnetism and Magnetic Materials*, in press.
3. K.V.O'Donovan, J.A.Borchers, C.F.Majkrzak, O.Hellwig, and E.E.Fullerton, *Physical Review Letters* **88**, 672011(2002).
4. H.Kepa, G.Springholz, T.M.Giebultowicz, K.I.Goldman, C.F.Majkrzak, P.Kacman, J.Blinkowski, S.Holl, H.Krenn, and G.Bauer, *Physical Review B*, in press.

HISTORY OF MAGNETIC MATERIALS

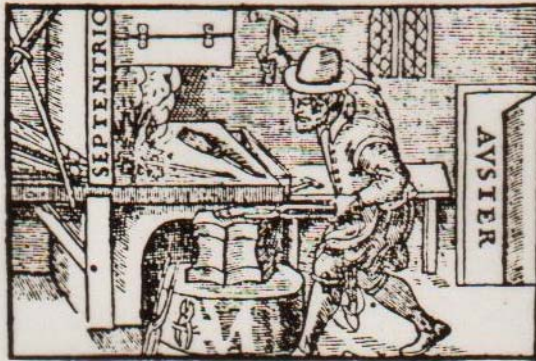
BN
(BEFORE NEUTRONS)

EMPIRICAL KNOWLEDGE

MACROSCOPIC

NATURAL PERMANENT MAGNETS : MAGNETITE (Fe_3O_4)

SEVERAL THOUSAND YEARS BC



1600 AD
GILBERT &
MAGNETIZED IRON

DEVELOPMENT OF ALNICO

1930's

1936 AD
DISCOVERY OF NEUTRON (AND m-DIFF)

AN
(ANNO NEUTRONI)

MORE SOPHISTICATED SCIENTIFIC UNDERSTANDING

MICROSCOPIC

CA 1950 AD

STRUCTURE;
LONG-RANGE ORDER

DYNAMICS;
COLLECTIVE EXCITATIONS

PHASE TRANSITIONS

FERRO MAGNETISM
ANTIFERROMAGNETISM
FERRIMAGNETISM
SPIRALS (PLANAR & CONICAL)
SPIN DENSITY WAVES
CHEMICALLY AMORPHOUS

SPIN WAVES
MAGNONS
FORCE OR STIFFNESS CONSTANTS

CRITICAL SCATTERING
CURIE, AND NEEL TEMPERATURES

DOMAINS
WALLS
ELECTRON MOMENT DISTRIBUTION WITHIN UNIT CELL

3D, 2D,
& 1D SYSTEMS

NEUTRON SCATTERING

MESOSCOPIC

CA 1980 →

EMPHASIS ON TECHNOLOGICAL APPLICATIONS OF THIN MAGNETIC FILMS : ENGINEERING MAGNETIC PROPERTIES

— INTERLAYER COUPLING & GIANT MAGNETO RESISTANCE (GMR) FOR READ HEADS

FUNDAMENTAL SCIENTIFIC INTEREST IN TWO CORRELATION LENGTH SCALES : e.g. Tb

Magnetic Neutron Scattering

Neutron:

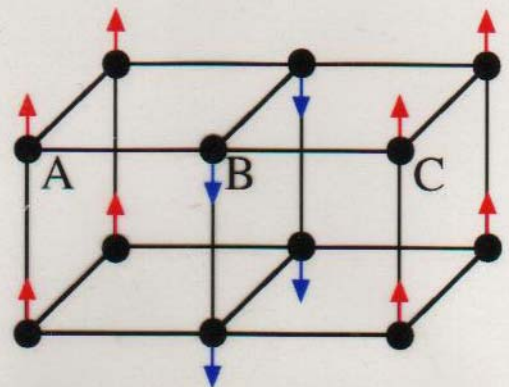
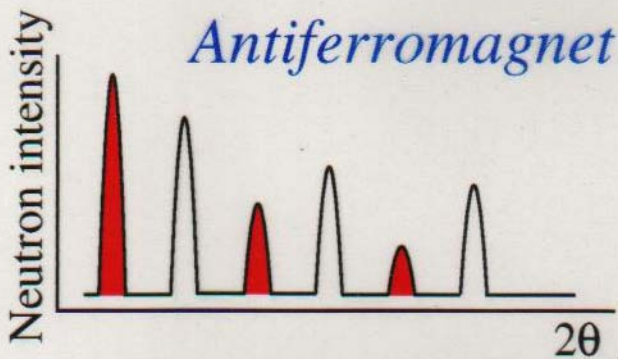
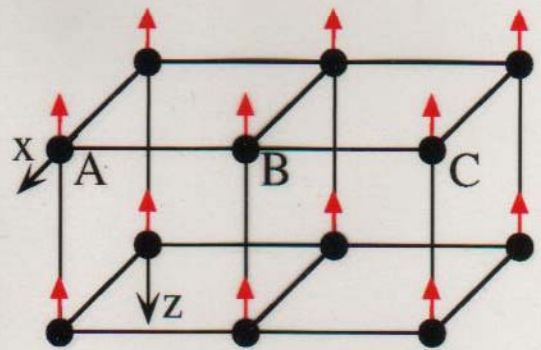
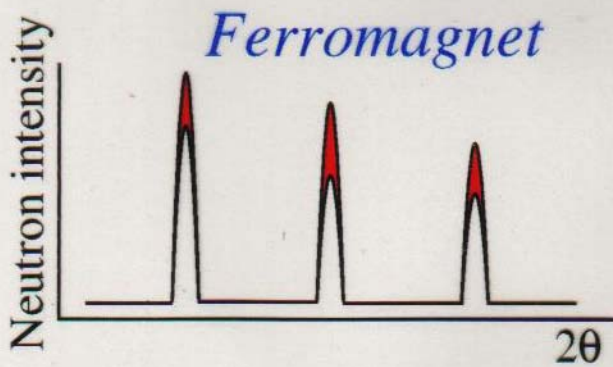
$$S = 1/2 ; \quad \mu = 1.91 \mu_N$$

Scattering by atomic

magnetic moments: $p = 0.54 \times S \times f(\sin\theta / \lambda) \times 10^{-12} \text{ cm}$

Magnetic and nuclear scattering amplitudes are of similar magnitude

DIFFRACTION BY MAGNETIC CRYSTALS

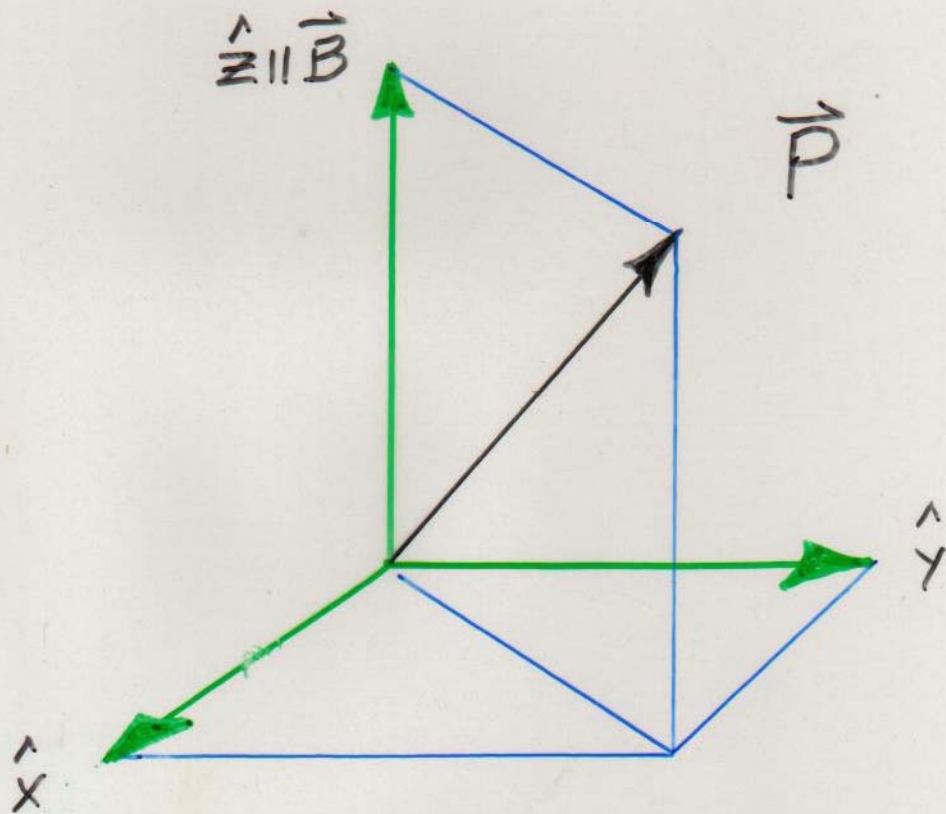


NEUTRON WAVE FUNCTION

$$\Psi = c_+ \begin{pmatrix} 1 \\ 0 \end{pmatrix} e^{i\vec{k}_+ \cdot \vec{r}} + c_- \begin{pmatrix} 0 \\ 1 \end{pmatrix} e^{i\vec{k}_- \cdot \vec{r}}$$

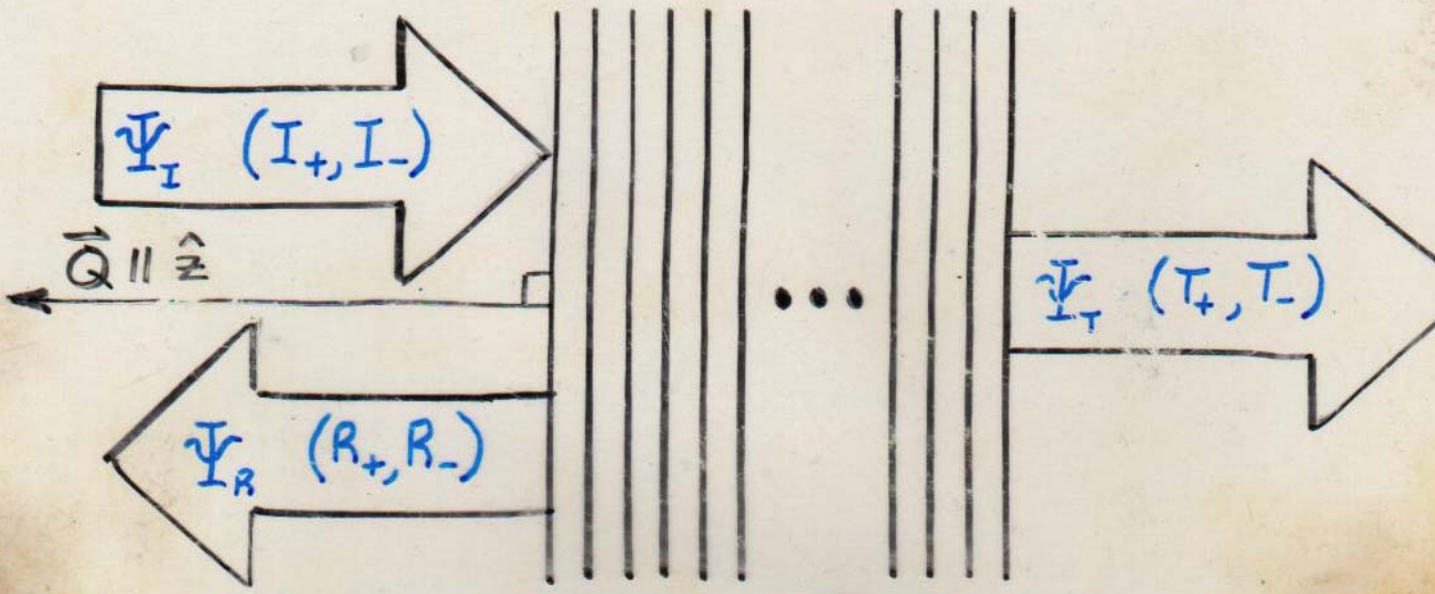
$$k_{\pm} = n_{\pm} k_0$$

$$n_{\pm}^2 = 1 - \frac{2m}{(\hbar k_0)^2} (V_N \pm \mu B)$$



CALCULATION FOR POLARIZED NEUTRONS

$$\left[\frac{-\hbar^2}{2m} \nabla^2 + (V-E) \right] \Psi = 0 \quad \Psi = \begin{pmatrix} \psi_+ \\ \psi_- \end{pmatrix}$$



$$V_N = Nb$$

$$V_M = -\vec{\mu} \cdot \vec{B}$$

$$\frac{\partial^2}{\partial z^2} \psi_+ + \left(\frac{Q^2}{4} - 4\pi\rho_{11} \right) \psi_+ - 4\pi\rho_{12} \psi_- = 0$$

$$\frac{\partial^2}{\partial z^2} \psi_- + \left(\frac{Q^2}{4} - 4\pi\rho_{22} \right) \psi_- - 4\pi\rho_{21} \psi_+ = 0$$

$$\rho_{11}^{(-)} = Nb + Np \sin\theta \sin\phi$$

$$\rho_{12}^{(+)} = Np (\cos\theta - i \sin\theta \cos\phi)$$

$$\begin{aligned}
\underline{V}_m &= -\underline{\mu} \cdot \underline{B} \\
&= -\gamma_m \left\{ \underline{S}_x B_x + \underline{S}_y B_y + \underline{S}_z B_z \right\} \\
&= -\gamma_m \frac{\hbar}{2} \left\{ \begin{pmatrix} 0 & B_x \\ B_x & 0 \end{pmatrix} + \begin{pmatrix} 0 & -iB_y \\ iB_y & 0 \end{pmatrix} + \begin{pmatrix} B_z & 0 \\ 0 & -B_z \end{pmatrix} \right\} \\
&= -\gamma_m \frac{\hbar}{2} \begin{pmatrix} B_z & B_x - iB_y \\ B_x + iB_y & -B_z \end{pmatrix} \\
&= \frac{\hbar^2}{2m\pi} \begin{pmatrix} N_{p_z} & N_{p_x} - iN_{p_y} \\ N_{p_x} + iN_{p_y} & -N_{p_z} \end{pmatrix}
\end{aligned}$$

- ONLY COMPONENTS OF $\underline{B} \perp \underline{Q}$ ARE EFFECTIVE IN SCATTERING NEUTRONS

$$\underline{\mu} = -\gamma_m \frac{\hbar}{2} \left\{ \begin{pmatrix} 0 & 1 \\ 1 & 0 \end{pmatrix} \hat{x} + \begin{pmatrix} 0 & -i \\ i & 0 \end{pmatrix} \hat{y} + \begin{pmatrix} 1 & 0 \\ 0 & -1 \end{pmatrix} \hat{z} \right\}$$

$$\begin{pmatrix} T_+ \\ T_- \\ i\frac{Q}{2}T_+ \\ i\frac{Q}{2}T_- \end{pmatrix} = \hat{M}_{\Pi} \begin{pmatrix} I_+ + R_+ \\ I_- + R_- \\ i\frac{Q}{2}[I_+ - R_+] \\ i\frac{Q}{2}[I_- - R_-] \end{pmatrix}$$

WHERE $|T_+|^2, |T_-|^2$ ARE THE TRANSMISSION PROBABILITIES

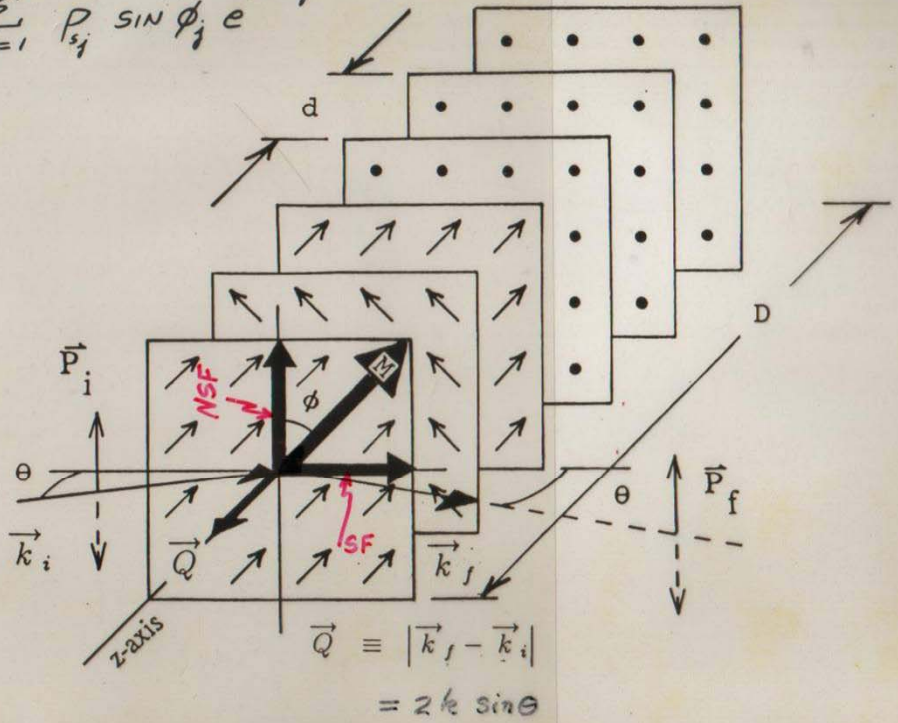
AND $|R_+|^2, |R_-|^2$ ARE THE REFLECTION PROBABILITIES

$$\hat{M}_{\Pi} = \prod_{l=L}^1 \hat{M}_l$$

(\hat{M}_l IS A 4x4 "TRANSFER" MATRIX CORRESPONDING TO THE l TH LAYER OF A MULTILAYER STRUCTURE)

$$F^{++} \propto \sum_{j=1}^N (b_{sj} \pm p_{sj} \cos \phi_j) e^{iQx_j}$$

$$F^{+-} \propto \sum_{j=1}^N p_{sj} \sin \phi_j e^{iQx_j}$$



SELECTION RULES FOR SCATTERING OF POLARIZED NEUTRONS BY MAGNETIC MOMENTS

- ONLY MAGNETIZATION COMPONENTS $\perp \vec{Q}$ GIVE RISE TO SCATTERING
- COHERENT NUCLEAR SCATTERING : ALL NSF
- NUCLEAR SPIN INCOHERENT

| <u>FIELD AT SAMPLE</u> | <u>SF</u> | <u>NSF</u> |
|-----------------------------|-----------|------------|
| $\vec{H} \parallel \vec{Q}$ | 2/3 | 1/3 |
| $\vec{H} \perp \vec{Q}$ | " | " |

- ANTIFERROMAGNET OR PARAMAGNET

| <u>FIELD AT SAMPLE</u> | <u>SF</u> | <u>NSF</u> |
|-----------------------------|-----------|------------|
| $\vec{H} \parallel \vec{Q}$ | 1 | 0 |
| $\vec{H} \perp \vec{Q}$ | 1/2 | 1/2 |

- SPIRAL MAGNETIC STRUCTURES WITH SINGLE DOMAIN OF ONE CHIRALITY :

$\vec{H} \parallel \vec{Q}$ $+\rightarrow-$ OR $-\rightarrow+$ SF ONLY,
DEPENDING ON WHETHER SPIRAL
IS RIGHT- OR LEFT-HANDED

$$\rho_s \equiv (\text{effective scattering length}) \cdot (\#\text{atoms/unit area})$$

$$\rho_v \equiv (\text{effective scattering length}) \cdot (\#\text{atoms/unit volume})$$

EXACT (DYNAMICAL)
HIGH REFLECTIVITY
LOW Q

BORN APPROXIMATION (KINEMATICAL)
LOW REFLECTIVITY
HIGH Q

$$|R|^2 = \left| \frac{4\pi}{Q} \int_0^L \Psi(Q, z) \rho_v(z) e^{i\frac{Q}{2}z} dz \right|^2$$

(CONTINUUM)

$$|R|^2 \simeq \left| \frac{4\pi}{Q} \int_0^L \rho_v(z) e^{iQz} dz \right|^2$$

(CONTINUUM)

To obtain $|R|^2$, solve corresponding pair of coupled wave equations for ψ_+ and ψ_- ($\Psi = \psi_+ + \psi_-$ in case of polarized beams) in piece-wise continuous fashion by imposing continuity of wave functions and their first derivatives at each boundary in a layered representation of the scattering medium. In each layer the scattering length density (scalar nuclear component and vector magnetic part) is taken to be constant. Each layer or slab can be characterized by a 4x4 matrix A_j . The spin-dependent reflectivities $|R|^2$, transmissions $|T|^2$, and incident beam (of polarization defined by I_+ and I_-) are then related by

$$|R|^2 \simeq \left| \frac{4\pi}{Q} \sum_{j=0}^{N-1} \rho_{sj}(z_j) e^{iQz_j} \right|^2$$

(DISCRETE ATOMIC PLANES)

Consider the particularly useful geometry where the neutron polarization axis and sample magnetizations are perpendicular to \vec{Q} : the effective coherent spin-dependent scattering lengths in this configuration are:

$$b_j + p_j \cos \phi_j \text{ (for } |R_{++}|^2 \text{)}$$

$$b_j - p_j \cos \phi_j \text{ (for } |R_{--}|^2 \text{)}$$

$$\text{and } p_j \sin \phi_j \text{ (for } |R_{+-}|^2 \text{ and } |R_{-+}|^2 \text{)}$$

where b_j is a nuclear scattering length and p_j is proportional to \vec{M}_j (scattering angle dependence of p_j is implicit).

$$\begin{pmatrix} T_+ \\ T_- \\ \frac{iQ}{2} T_+ \\ \frac{iQ}{2} T_- \end{pmatrix} = \prod_{j=N}^1 A_j \begin{pmatrix} I_+ + R_+ \\ I_- + R_- \\ \frac{iQ}{2} [I_+ - R_+] \\ \frac{iQ}{2} [I_- - R_-] \end{pmatrix}$$

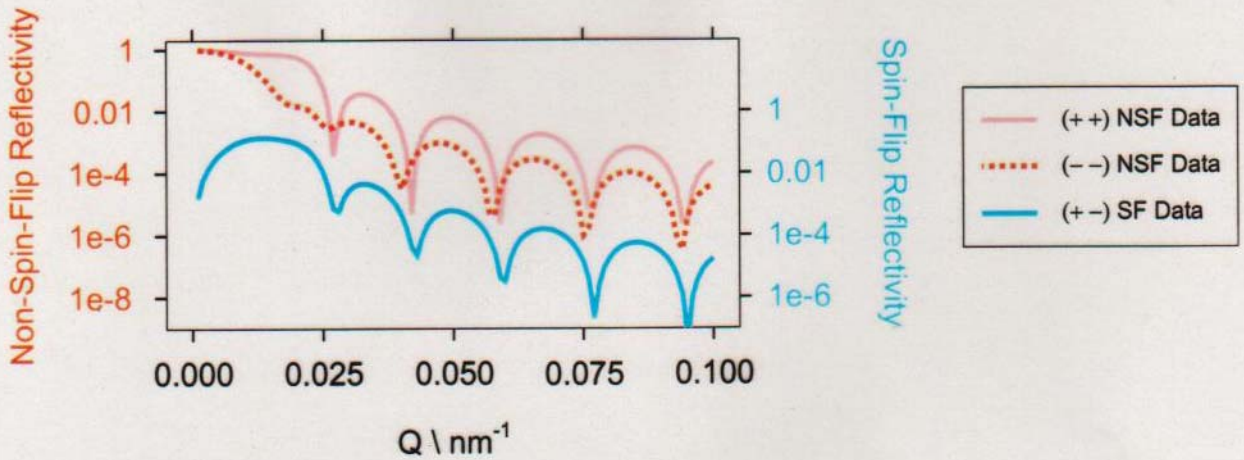
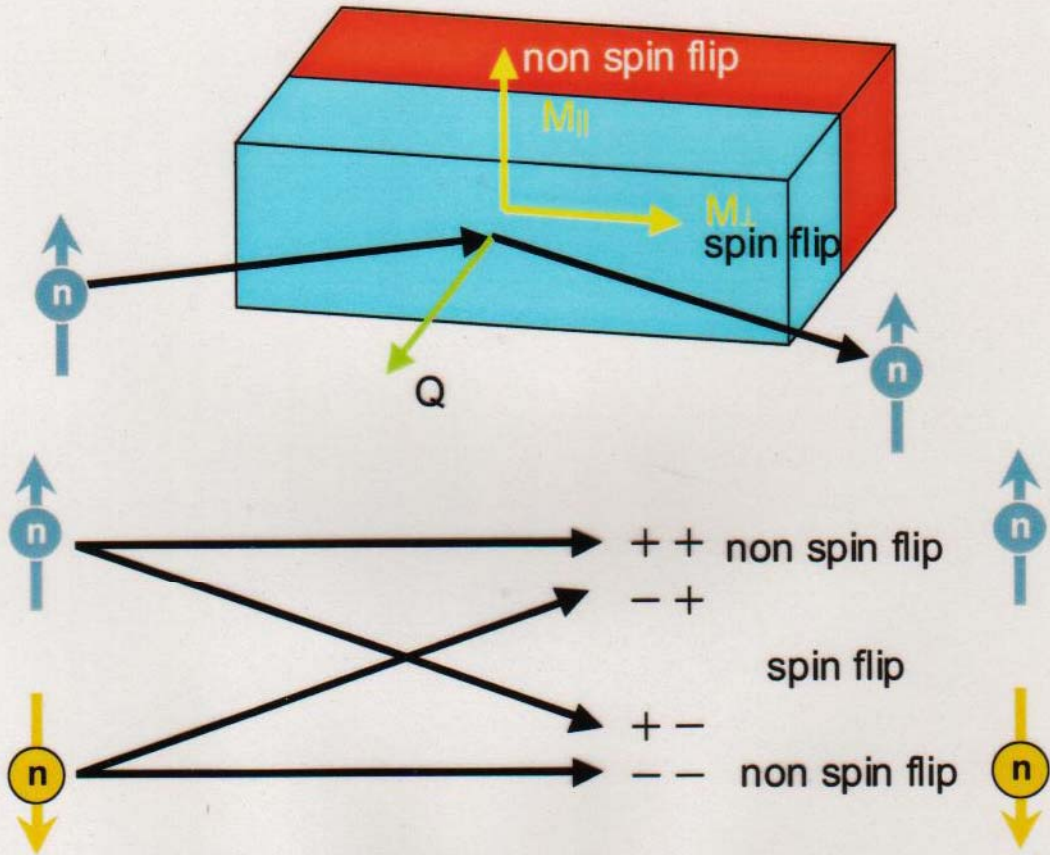
Note: a) substrates should be included in above matrix equation if present;
and b) the component of \vec{B} or \vec{M} perpendicular to the interface must be continuous as required by Maxwell's equations. Thus, only in-plane components of \vec{B} result in specular scattering.

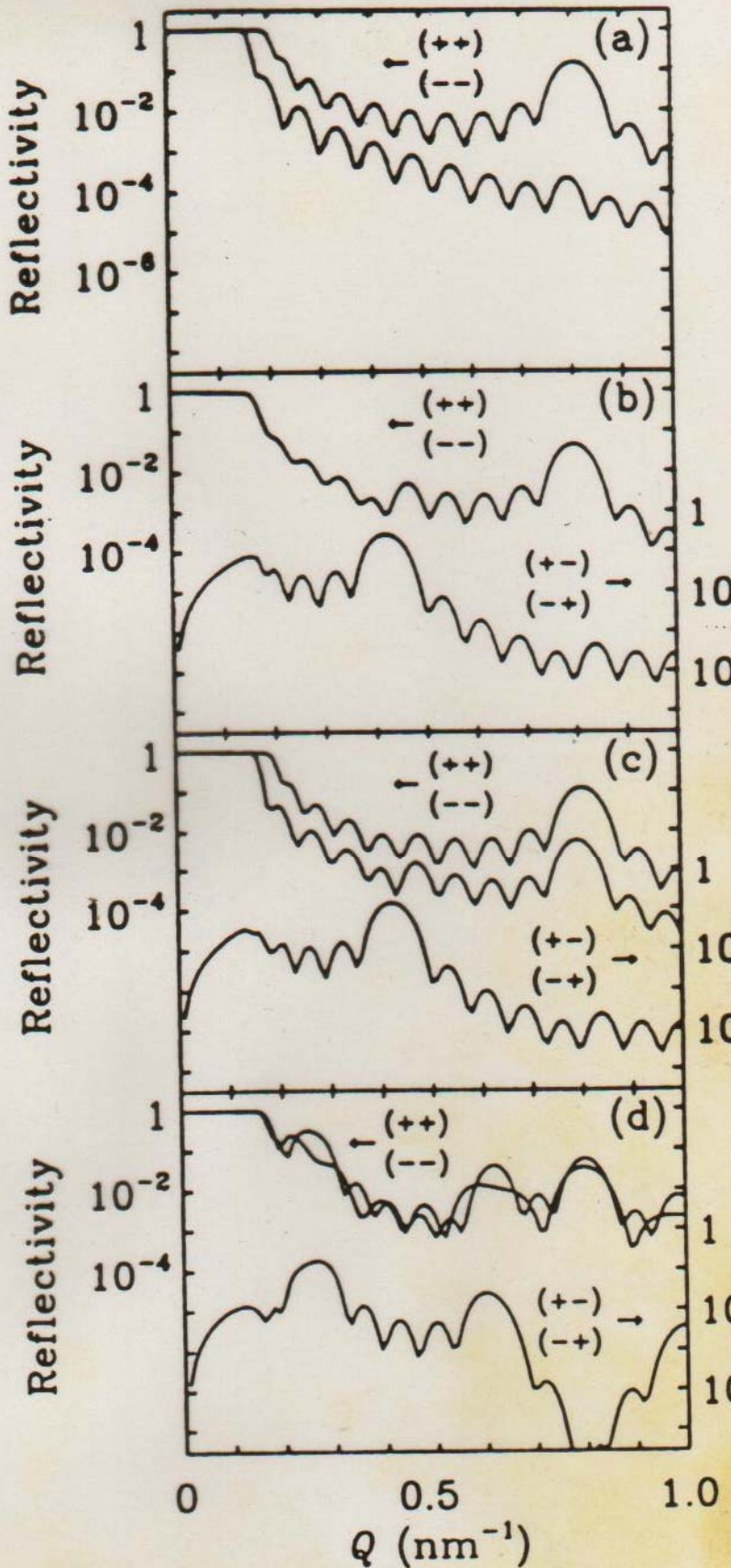
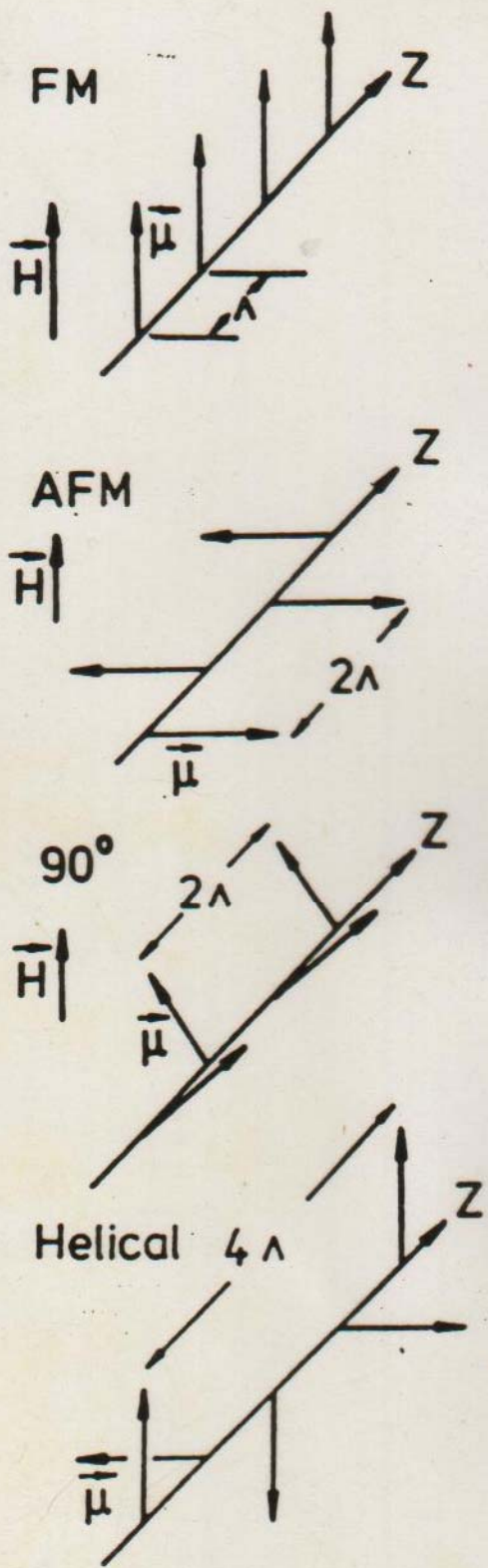
Note: a) for a periodic superlattice, the sum over all N atomic planes can be replaced with a sum over a single unit cell multiplied by the factor $\sin(MQD/2)/\sin(QD/2)$ where M is the number of unit cells and D is the thickness of a cell; and b) Debye-Waller factors which take into account the effects of thermal vibrations have not been included.

Polarized Neutron Reflectometry

at the NCNR NG-1 Reflectometer

Scattering experiment determines the correlation of magnetism at two depths separated by $d \sim 2\pi/Q$





ANKNER, SCHREYER,
MAJKRZAK, ZABEL, et al.

Polarization Analysis of Thermal-Neutron Scattering*

R. M. MOON, T. RISTE,† AND W. C. KOEHLER

Solid State Division, Oak Ridge National Laboratory, Oak Ridge, Tennessee 37830

(Received 30 December 1968)

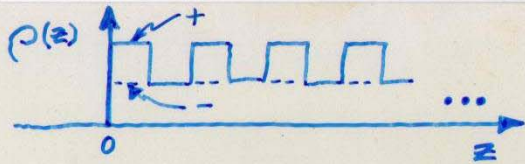
A triple-axis neutron spectrometer with polarization-sensitive crystals on both the first and third axes is described. The calculation of polarized-neutron scattering cross sections is presented in a form particularly suited to apply to this instrument. Experimental results on nuclear incoherent scattering, paramagnetic scattering, Bragg scattering, and spin-wave scattering are presented to illustrate the possible applications of neutron-polarization analysis.

I. INTRODUCTION

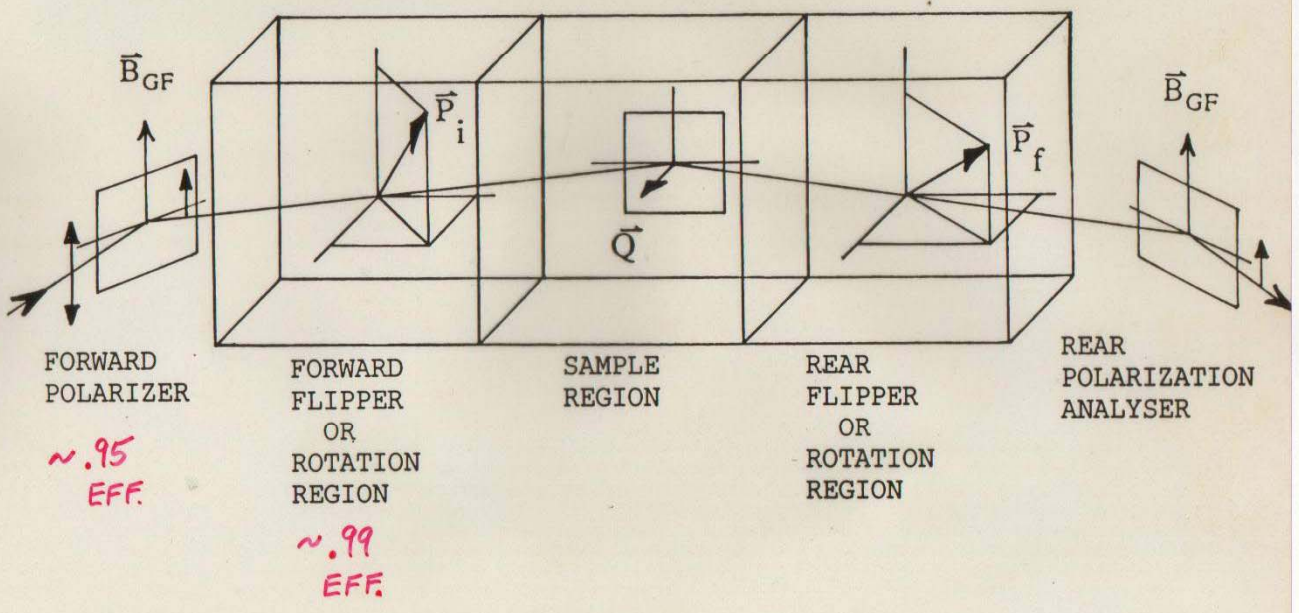
WE have added a new dimension to measurements of thermal-neutron scattering by constructing, at the Oak Ridge High-Flux Isotope Reactor, a triple-axis spectrometer with polarization-sensitive crystals on both the first and third axes. With this instrument the distribution of scattered neutrons from an initially monochromatic, polarized beam is measured as a

scattering ($++$ and $--$). The theoretical quantities of greatest interest are the partial cross sections.

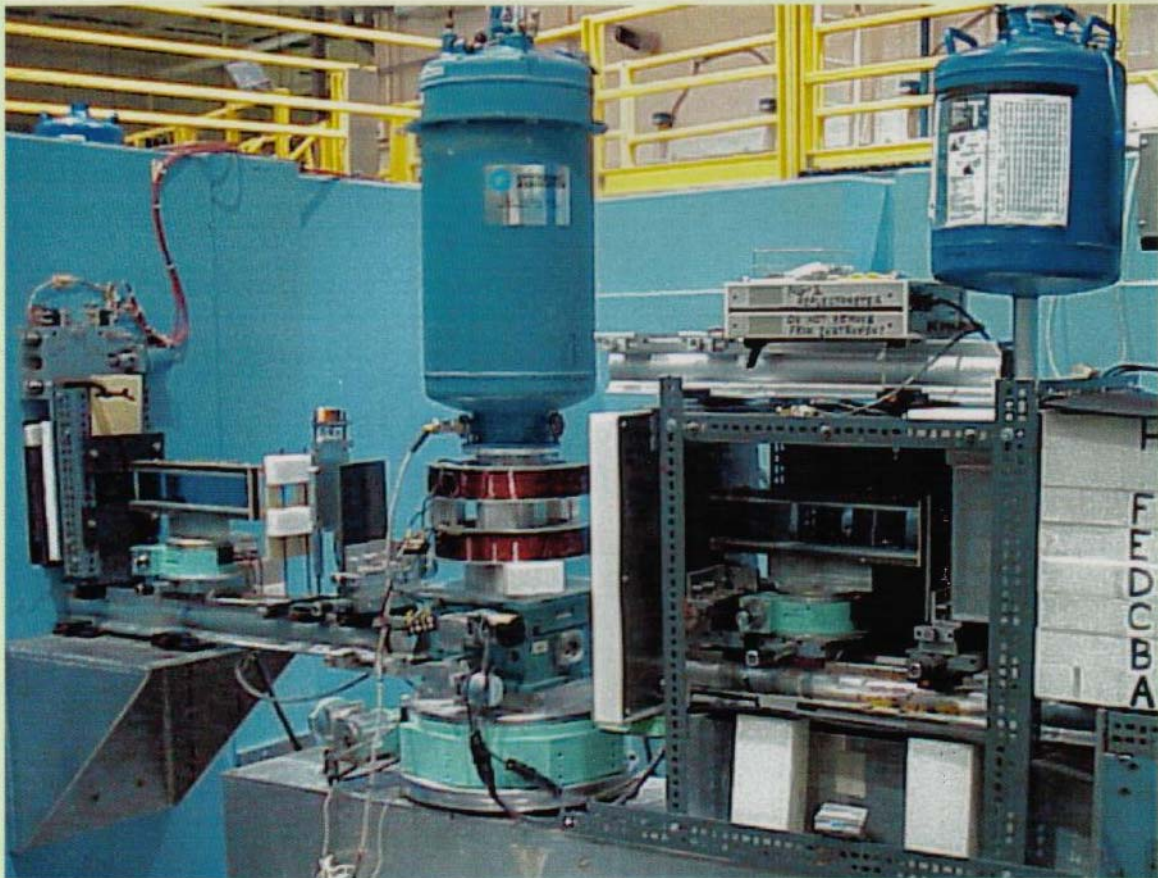
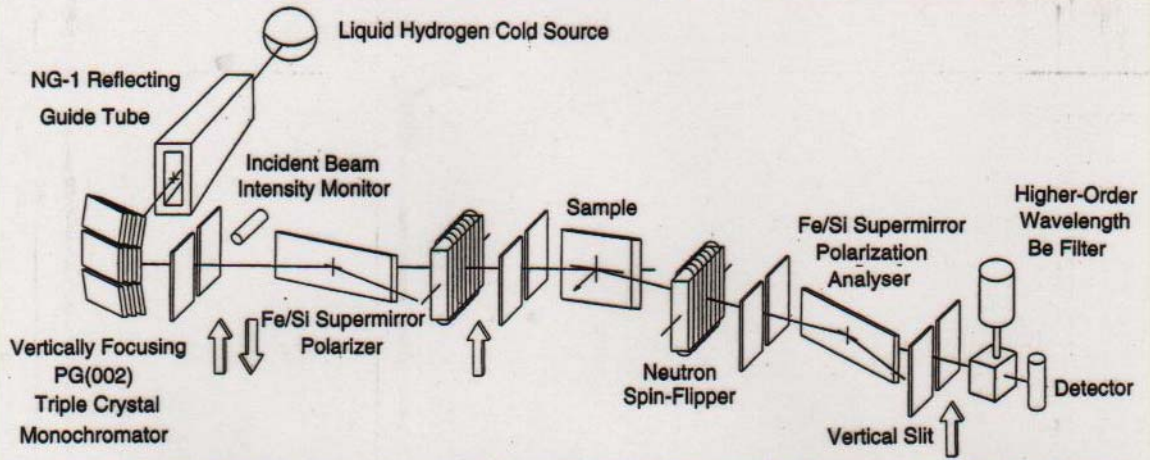
This is a different language than is customarily used by theoreticians in describing the scattering of polarized neutrons. The total cross section (summed over final spin states) and the final polarization are calculated as a function of the initial polarization. The polarization equation is a vector relationship giving the magnitude and direction of the final polarization. We measure



$$|F_{\pm}|^2 \propto |N_b \pm N_p|^2$$

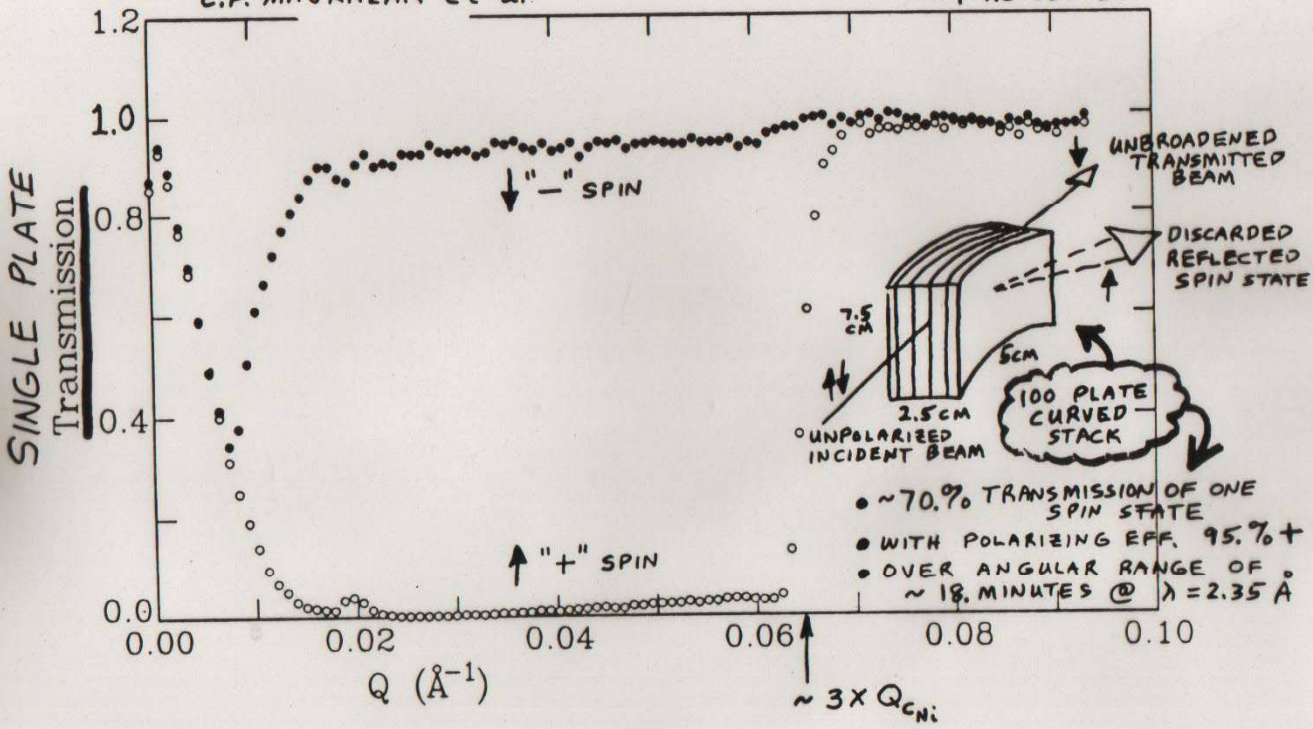
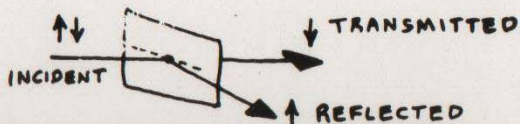


NIST Center for Neutron Research Polarized Neutron Reflectometer



MEASURED ON BT 7
POLARIZED BEAM REFLECTOMETER
AT NIST

C.F. MAJKRZAK et al.



Fe/Si SUPERMIRROR POLARIZER IN TRANSMISSION (SINGLE CRYSTAL Si SUBSTRATE)
(COATING MANUFACTURED BY OSMC COMPANY - J. WOOD)

Figure B

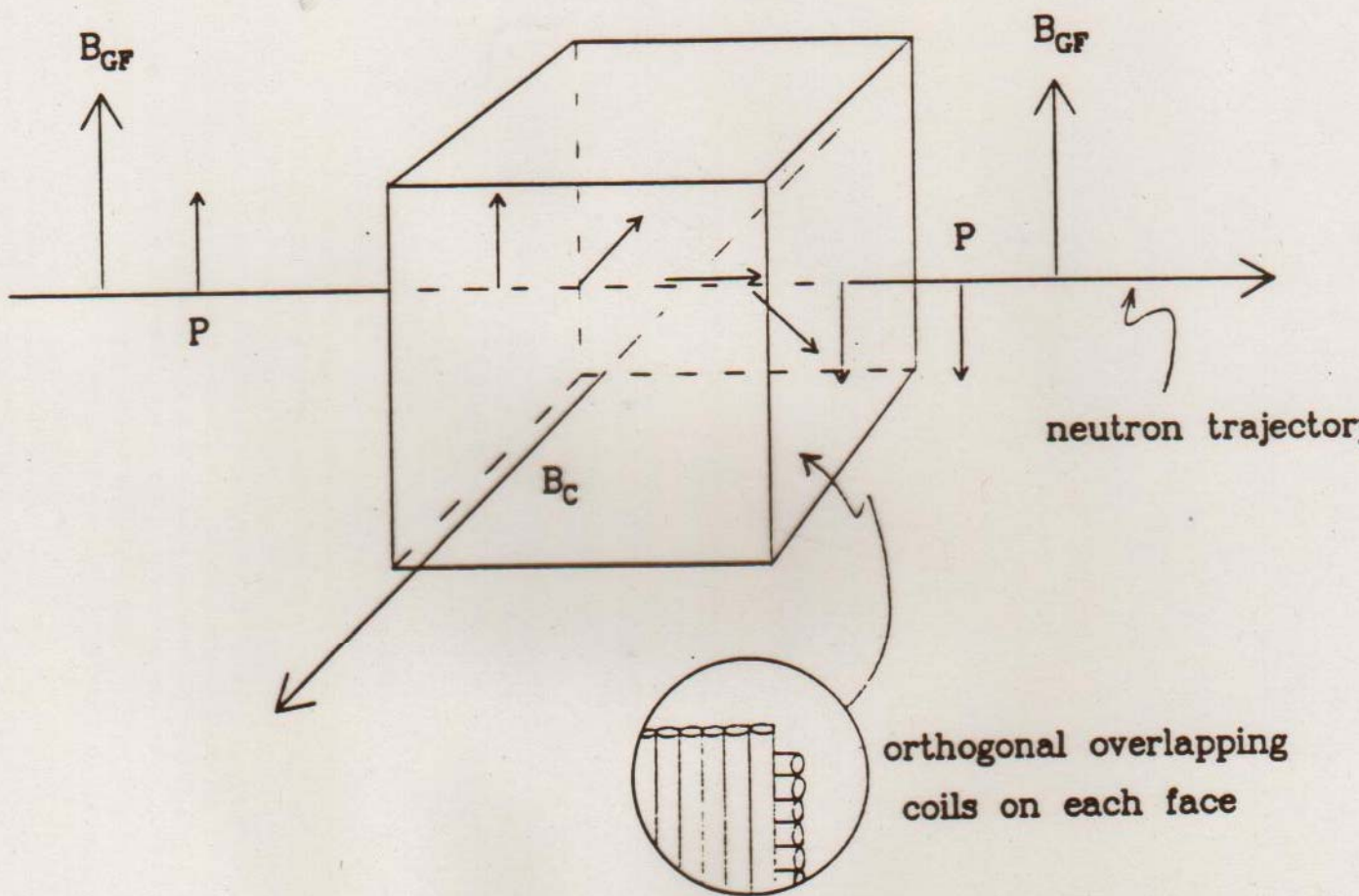


Fig. 5-2

Figure 5-2. Cubic volume defined by three mutually orthogonal, intersecting solenoidal coils of square cross section within which a magnetic field \vec{B}_c is created. Assuming sudden transitions across the coil boundaries, the neutron polarization will precess about the different field direction inside the coil as described in the text. Thus, the neutron polarization \vec{P} can be rotated to any general orientation in space relative to the guide field \vec{B}_{GF} .

TABLE 2: POLARIZING AND FLIPPING EFFICIENCY CORRECTIONS

$\sigma_{++}, \sigma_{--}, \sigma_{+-}$, and σ_{-+} are defined as the NSF and SF reflectivities, respectively, corresponding to the sample.

$I^{off\ off}$, $I^{on\ on}$, $I^{off\ on}$, and $I^{on\ off}$ are defined as the intensities measured with front and rear flippers respectively, in "on" (π rotation of the neutron spin) or "off" (no rotation) states.

F, R, f, and r are defined as the front and rear polarizer and front and rear flipper efficiencies, respectively.

The relationship between the intensities measured in the detector and the sample spin-dependent reflectivities are [28]

$$\begin{aligned} I^{off\ off}/\beta &= \sigma_{++}(1+F)(1+R) & I^{on\ off}/\beta &= \sigma_{++}(1+R)[1+F(1-2f)] \\ &+ \sigma_{-+}(1-F)(1+R) & &+ \sigma_{-+}(1+R)[1-F(1-2f)] \\ &+ \sigma_{--}(1-F)(1-R) & &+ \sigma_{--}(1-R)[1-F(1-2f)] \\ &+ \sigma_{+-}(1+F)(1-R) & &+ \sigma_{+-}(1-R)[1+F(1-2f)] \end{aligned}$$

$$\begin{aligned} I^{off\ on}/\beta &= \sigma_{++}(1+F)[1+R(1-2r)] & I^{on\ on}/\beta &= \sigma_{++}[1+F(1-2f)][1+R(1-2r)] \\ &+ \sigma_{-+}(1-F)[1+R(1-2r)] & &+ \sigma_{-+}[1-F(1-2f)][1+R(1-2r)] \\ &+ \sigma_{--}(1-F)[1-R(1-2r)] & &+ \sigma_{--}[1-F(1-2f)][1-R(1-2r)] \\ &+ \sigma_{+-}(1+F)[1-R(1-2r)] & &+ \sigma_{+-}[1+F(1-2f)][1-R(1-2r)] \end{aligned}$$

The spin-dependent reflectivities can be solved for from the measured intensities if the instrumental polarizing and flipping efficiencies and the constant β are determined.

The constant β is given by

$$2\beta = \frac{I_{NS}^{on\ on} I_{NS}^{off\ off} - I_{NS}^{on\ off} I_{NS}^{off\ on}}{I_{NS}^{on\ on} + I_{NS}^{off\ off} - I_{NS}^{on\ off} - I_{NS}^{off\ on}} \equiv \alpha$$

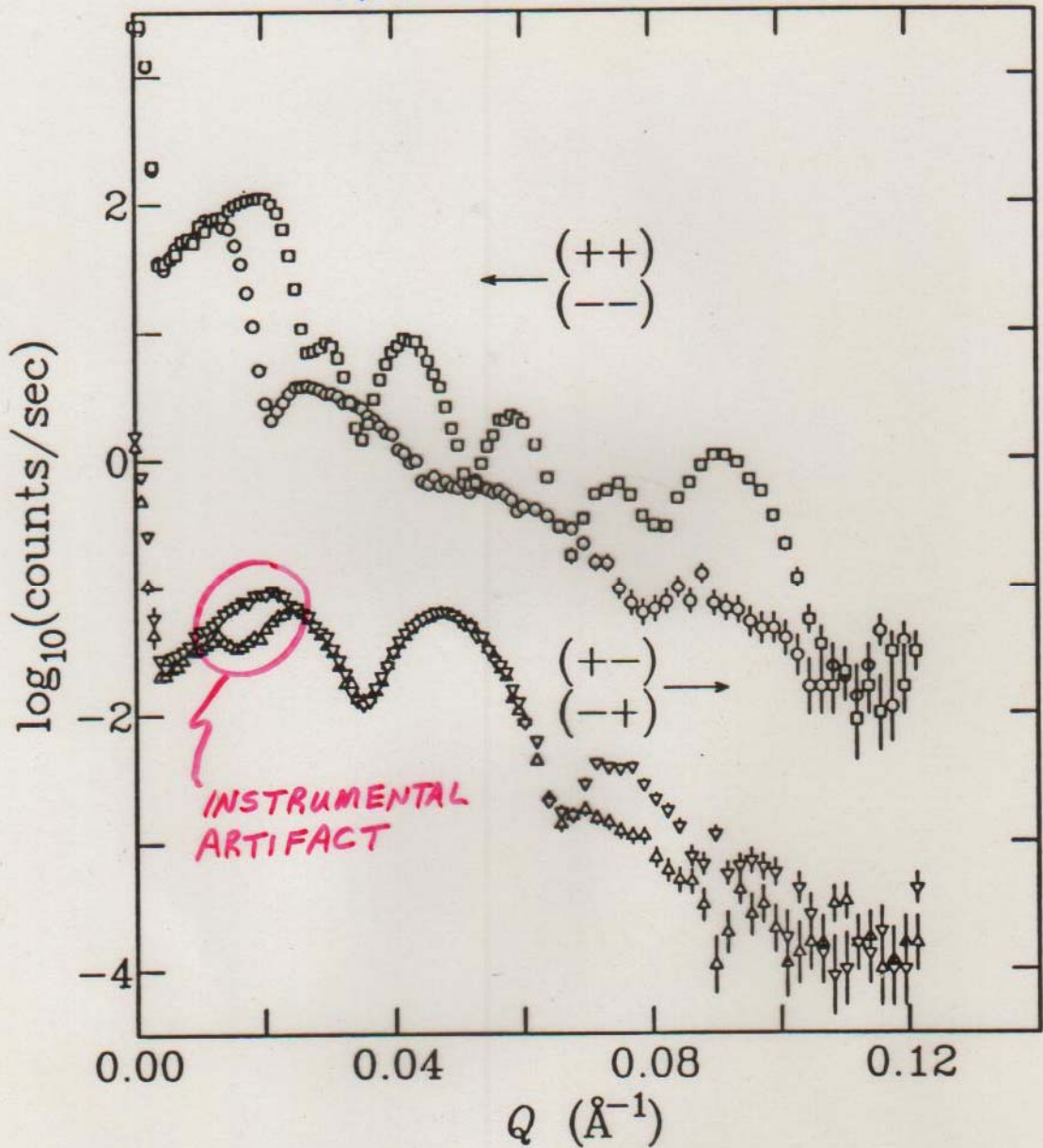
where the subscript "NS" signifies measurements at zero scattering angle with "no sample" in place. Also,

$$\begin{aligned} I_{NS}^{off\ off}/\alpha &= FR + 1 \\ I_{NS}^{on\ off}/\alpha &= FR(1-2f) + 1 \\ I_{NS}^{off\ on}/\alpha &= FR(1-2r) + 1 \end{aligned}$$

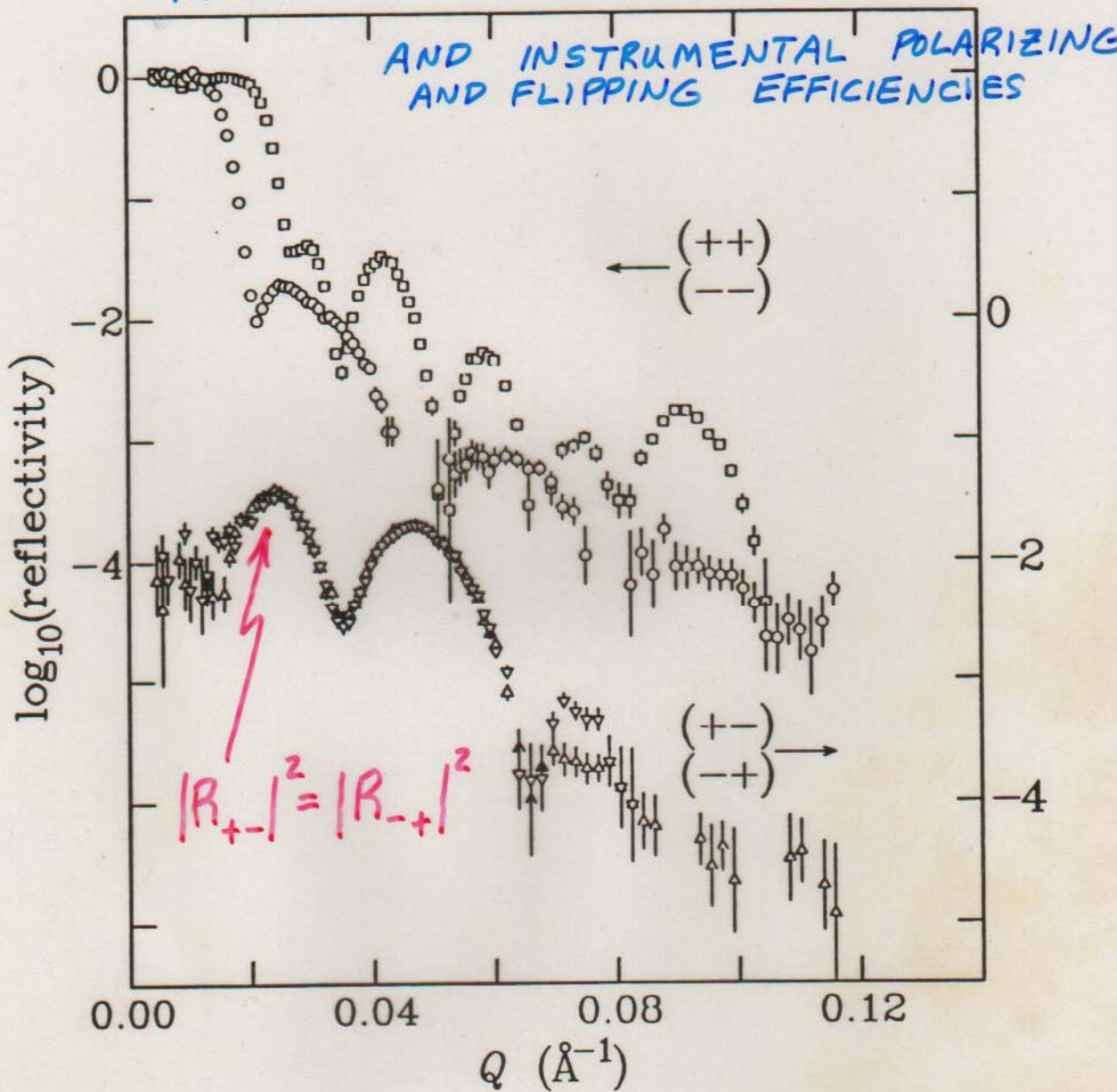
so that f, r, and the product FR can be determined.

If the sample is replaced with a "reference sample" (RS) which has $\sigma_{++} \neq \sigma_{--}$ and $\sigma_{+-} = \sigma_{-+} = 0$ (σ_{++} and σ_{--} need not be known), then F and R can be individually determined.

Fe/Cr SUPERLATTICE : UNCORRECTED
REFLECTED INTENSITIES



Fe/Cr SUPERLATTICE : REFLECTIVITIES
AFTER CORRECTION FOR BEAM FOOTPRINT



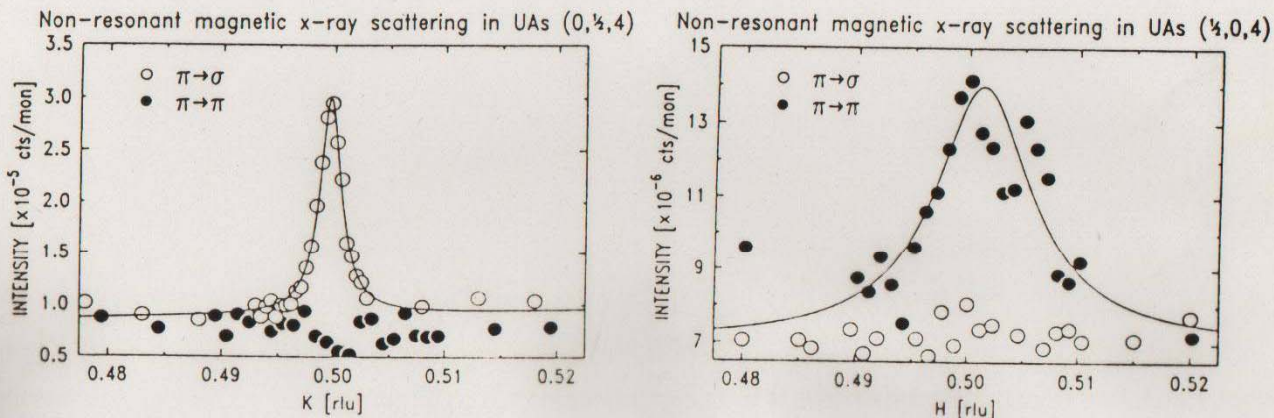


Fig. 2: Experimental results taken with different polarization (as indicated) for the satellites around the (004) charge peak in UAs. Based on Eq. (4) and our understanding of the magnetic structure (from neutrons) the structure factors are proportional to:

$$\begin{array}{ll}
 \text{left hand side:} & (\pi \rightarrow \pi) \quad \underline{\text{zero}} \quad (\pi \rightarrow \sigma) \quad \underline{(L + S)} \\
 \text{right hand side:} & (\pi \rightarrow \pi) \quad \underline{(\sim 0.5L + S)} \quad (\pi \rightarrow \sigma) \quad \underline{(-0.1 S)}
 \end{array}$$

(AFTER G. LANDER *et al.*)

- γ -rays DO interact with magnetic as well as with electronic charge distributions

- for γ -rays, $\frac{I_{\text{MAGN.}}}{I_{\text{CHARGE}}} \sim 10^{-6}$

→ magn. scatt. of γ -rays is a relativistic effect)

(non-resonant)

- $V_{\text{CHARGE}} \propto FT(\text{charge density}) \cdot C$

$V_{\text{MAGN.}} \propto \frac{1}{2} FT(\text{orbital density}) \cdot A$
 $+ FT(\text{spin density}) \cdot B$

where A, B, & C give the pol. dep. of the scattering

- for neutrons, $\mu \propto \mu_B (L+2S)$ so that L & S contr. can't be directly separated (because spatial extents of magn. dens. of L & S contrib. are diff., modelling & fitting allows for separation)

- resonant magnetic x-ray scatt.:

e.g. in Ho at an x-ray energy near the L(III) absorption edge, the inc. photon excites a 3p electron to the 5d unoccupied level - under these conditions electric 2^+ pole resonances are stimulated and contribute to the coherent scattering amplitude! can roughly describe this process as one in which a core electron is excited to an unoccupied level and forms a magnetic resonance with the unpaired electrons in that particular shell

- resonant enhancement as large as 10^6 !

- resonant magn. scatt. is element specific

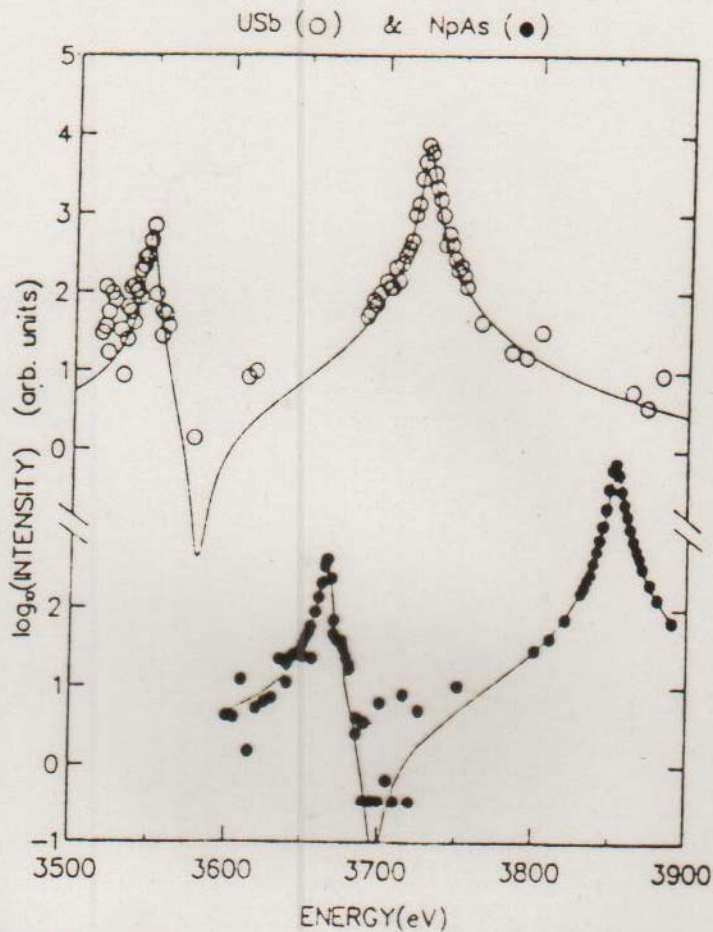


Fig. 3: Intensity of the magnetic satellite from a uranium and neptunium compound as a function of energy. The solid lines are fits to atomic resonance theory. (Taken from Ref. 24 and 25)

(D. GIBBS
et al.)

(G. LANDER
et al.)

SOFT X-RAY · MAGNETIC
CIRCULAR DICHOISM

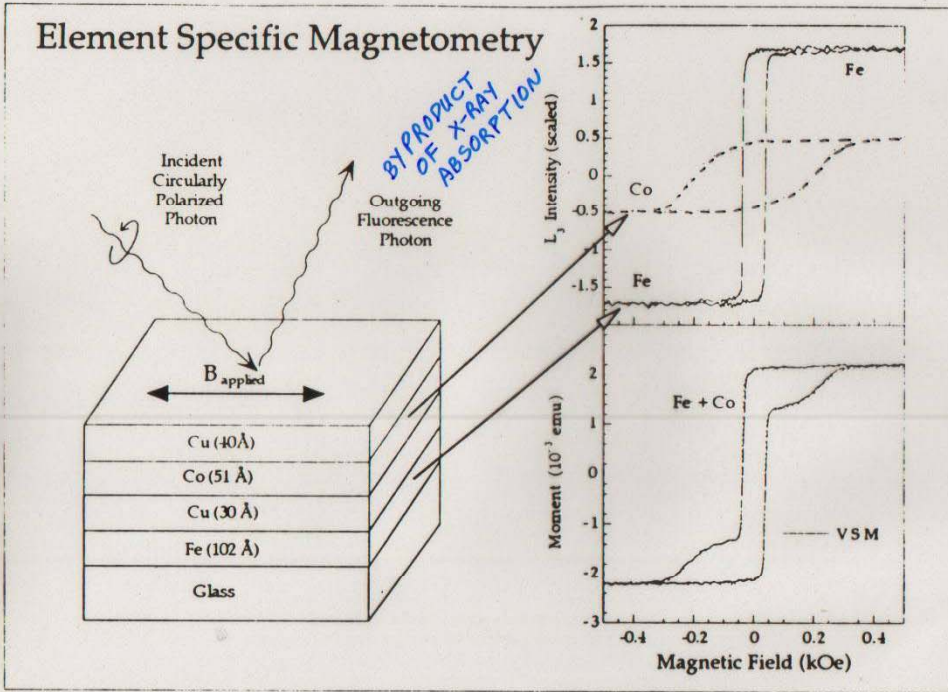


Figure 3. Element specific magnetometry. Multilayer structure (left) indicates the hysteresis loop (top right) associated with Fe (solid) and Co (dashed) measured from the resonant L_2 white-line intensity vs. applied field for comparison (bottom right) of summed Fe+Co (dashed) with total moment (solid) hysteresis loop.

(Y. IDZERDA
et al.)

ABSORPTION OF
CIRCULARLY
POLARIZED
PHOTONS AT
MAGNETICALLY
INTERESTING
 $2p \rightarrow 3d$
TRANSITIONS IS AN
ELEMENT SPECIFIC
PROBE OF
MAGNETIC ORDER
AND STRUCTURE

PHOTON "SPIN"

(RT. OR LT. CIRCULAR
POL.)

ALIGNED OR ANTI-
ALIGNED TO ELECTRON
SPIN